PEGylated Paclitaxel Nanomedicine Meets 3D Confinement: Cytotoxicity and Cell Behaviors

Wenhai Lin[1], Yuanhao Xu[1], Xiao Hong[1], and Stella Pang [1]

[1]City University of Hong Kong

July 13, 2022

Abstract

It is beneficial to investigate the effect of nanomedicines on cancer cell behaviors on three-dimensional (3D) platforms for evaluating and developing novel antitumor nanomedicines *in vitro*. Two-dimensional flat surface is widely used to study the cytotoxicity of nanomedicines on cancer cells, and there is little work using 3D confinement to assess the effect of nanomedicine on cancer cells. In this work, PEGylated paclitaxel nanoparticles (PEG-PTX NPs) were applied for the first time to treat nasopharyngeal carcinoma (NPC43) cells in 3D confinement which consisted of microwells with different sizes and a glass cover. The cytotoxicity of the small molecule drug paclitaxel (PTX) and PEG-PTX NPs were studied in microwells with sizes of 50×50, 100×100, and 150×150 μm^2 and with covers. After NPC43 cells were treated with PTX and PEG-PTX NPs, the cell migration speed and cell morphology were analyzed in different microwells without and with covers. The relationship between the cytotoxicity from drugs, the size effect from microwells, and cell behaviors were analyzed. These results not only show the effect of 3D confinement on cytotoxicity of nanomedicines and cell behaviors, but also provide a novel method to screen anticancer drugs and evaluate the cell behaviors *in vitro*.

PEGylated Paclitaxel Nanomedicine Meets 3D Confinement: Cytotoxicity and Cell Behaviors

Wenhai Lin#, Yuanhao Xu#, Xiao Hong, and Stella W. Pang*

#These authors contributed equally

*Corresponding Author

Dr. W. Lin, Dr. Y. Xu, X. Hong and Prof. S. W. Pang

Department of Electrical Engineering

City University of Hong Kong

Hong Kong, China E-mail: pang@cityu.edu.hk

Keywords: nanomedicine, microwell, paclitaxel, cell migration, 3D confinement

It is beneficial to investigate the effect of nanomedicines on cancer cell behaviors on three-dimensional (3D) platforms for evaluating and developing novel antitumor nanomedicines *in vitro* . Two-dimensional flat surface is widely used to study the cytotoxicity of nanomedicines on cancer cells, and there is little work using 3D confinement to assess the effect of nanomedicine on cancer cells. In this work, PEGylated paclitaxel nanoparticles (PEG-PTX NPs) were applied for the first time to treat nasopharyngeal carcinoma (NPC43) cells in 3D confinement which consisted of microwells with different sizes and a glass cover. The cytotoxicity of the small molecule drug paclitaxel (PTX) and PEG-PTX NPs were studied in microwells with sizes of 50×50, 100×100, and 150×150 μm^2 and with covers. After NPC43 cells were treated with PTX and PEG-PTX NPs, the cell migration speed and cell morphology were analyzed in different microwells without and

with covers. The relationship between the cytotoxicity from drugs, the size effect from microwells, and cell behaviors were analyzed. These results not only show the effect of 3D confinement on cytotoxicity of nanomedicines and cell behaviors, but also provide a novel method to screen anticancer drugs and evaluate the cell behaviors *in vitro* .

1. Introduction

Nanoparticles (NPs) are widely used for many applications including catalysis, medicine, and sensors.[1-9]Nanoparticles applied in medicine, or nanomedicines, can overcome various limitations of small molecule drugs such as strong hydrophobicity, poor bioavailability, and big side effects.[10-20] Some nanomedicines have been available for clinical use, and many other nanomedicines are under clinical evaluation.[21, 22] Among these nanomedicines, two nanomedicines based on paclitaxel (PTX), marketed as Abraxane and Genexol-PM, are widely used in clinics for treating various cancers such as ovarian, head and neck, and non-small cell lung cancers.[22-26] To achieve successful preclinical evaluation of nanomedicines, three-dimensional (3D) platforms are more suitable as the common two-dimensional (2D) cell culture platforms on flat surface cannot mimic the complex 3D microenvironment *in vivo* .

To better test the cytotoxicity of small molecule drugs and nanomedicines *in vitro* , some 3D platforms were used.[27-39] Microwells were extensively used in cancer cell studies including immune cell meditated cancer treatment and anti-cancer drug response evaluation.[40-42]Microwells have also been used for help cancer cells to form spheroids to test the cytotoxicity of nanomedicines.[43, 44]However, most of these studies still focused on the collective influence of nanomedicines on the cancer cell population. Previous works have revealed a clear dependence of cancer cell susceptibility to treatments with the microwell sizes.[45, 46] Therefore, it is important to evaluate the effect of physical confinement by microwells on the effectiveness of nanomedicines in a single-cell level, such that the time dependent nanomedicine treatment on individual cancer cell could be better understood. To the best of our knowledges, this is the first study using 3D confinement with the cover on the top to evaluate the cytotoxicity of nanomedicine and cell behaviors after cancer cells are treated with nanomedicines.

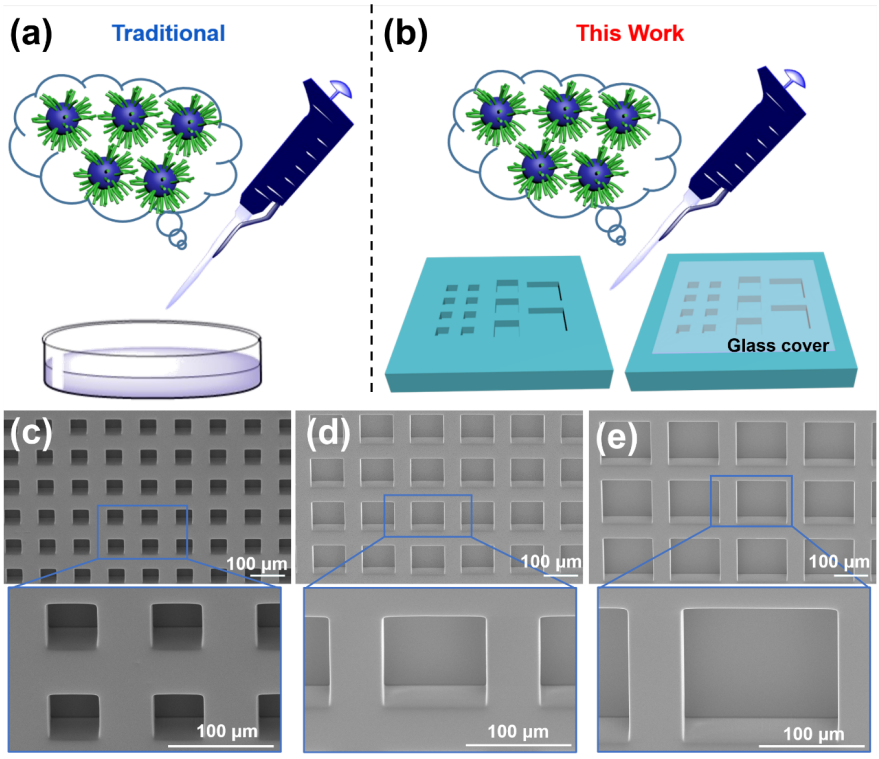

Figure 1 . Schematic illustration to study effect of nanomedicines on cell behaviors and cytotoxicity on (a) flat surface and (b) 3D platforms of microwell arrays without and with glass cover. Scanning electron micrographs of (c) 50×50 μm^2, (d) 100×100 μm^2, and (e) 150×150 μm^2 polydimethylsiloxane microwells.

Typically, 2D flat surface such as a petri dish is used to study the effect of nanomedicines on cell behaviors as shown in **Figure. 1a** . In this work, 3D platforms consisted of microwells with different sizes of 50×50, 100×100, and 150×150 μm^2 and with glass covers were used as shown in Figure. 1b. The cover provided the microwells additional confinement on the top. The microwells had flat rather than curved bottoms such that the migratory behavior of cells could be evaluated. PEGylated paclitaxel nanoparticles (PEG-PTX NPs) as the nanomedicine were applied for the first time to treat nasopharyngeal carcinoma (NPC43) cells in microwells without and with a cover. In microwells without and with the cover, NPC43 cells showed different cell behaviors such as cell proliferation, cell migration speed, cell elongation, and cell spreading area. Furthermore, the effect of microwells and 3D confinement on the cytotoxicity of PTX and PEG-PTX NPs was studied in detail.

2. Results and Discussion

2.1. Characterization of microwells and PEG-PTX NPs

Polydimethylsiloxane (PDMS) microwells arrays were fabricated according to our previous work.[47]Microwells with different sizes of 50×50, 100×100, and 150×150 μm^2 as shown in Figure. 1c-e were fabricated. The depth of all the microwells were 50 μm and the space between adjacent microwells was 50 μm. These microwells were used as 3D platforms to evaluate the effect of PEG-PTX nanomedicine on NPC43 cells.

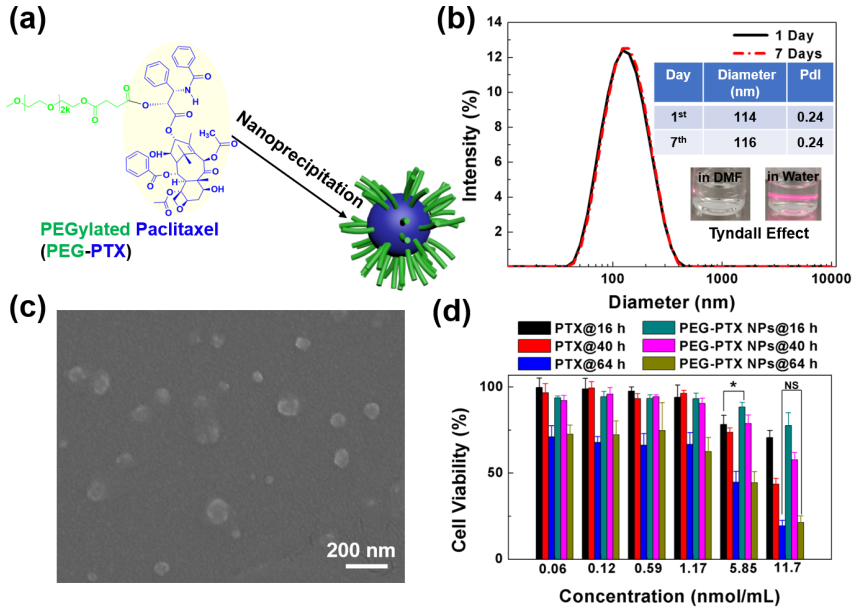

Figure 2 . Characterization of PEGylated paclitaxel nanoparticles (PEG-PTX NPs). (a) Schematic illustration of PEG-PTX NPs synthesis. (b) Size distribution and 7-day stability of PEG-PTX NPs measured by dynamic light scattering. Inserted images: PEG-PTX dissolved in dimethylformamide (left) and PEG-PTX NPs in water (right). (c) Scanning electron micrographs of PEG-PTX NPs. (d) Cell viability of NPC43 cells treated with PTX and PEG-PTX NPs for 16, 40, and 64 h, respectively. One-way ANOVA and Tukey's post hoc tests, NS – not significant and *p <0.05.

PEG-PTX was synthesized according to previously reported work.[48-50] PEG is hydrophilic and PTX is

hydrophobic so the amphiphilic PEG-PTX could self-assemble into nanoparticles (PEG-PTX NPs) in water by the nanoprecipitation method as shown in **Figure. 2a** . The diameter and polydispersity index (PdI) of PEG-PTX NPs were measured by dynamic light scattering (DLS). As shown in Figure. 2b, the diameter and PdI of PEG-PTX NPs were 114 nm and 0.24, respectively. After storing at room temperature for 7 days, the diameter and PdI of PEG-PTX NPs remained unchanged, which showed that the synthesized PEG-PTX NPs were stable. As shown in the inserted photos of Figure. 2b, PEG-PTX NPs in water showed the clear Tyndall effect as a bright light path in water was observed when irradiated by a laser, which indicated that nanoparticles were successfully synthesized in water. However, PEG-PTX could be dissolved in dimethylformamide (DMF) so there were no nanoparticles or Tyndall effect in DMF. The morphology of PEG-PTX NPs was revealed by a scanning electron microscope (SEM). As shown in Figure. 2c, the diameter of some PEG-PTX NPs was below 100 nm. Overall, the PEG-PTX NPs had a little smaller size than that measured by DLS as shown in Figure. 2b because the hydration layer was used in DLS but the dry sample was used in SEM. These results demonstrated that stable PEG-PTX NPs were successfully formed for the biological experiments.

2.2. Cytotoxicity of PEG-PTX NPs in microwells

PTX is a clinical anticancer drug and it can be used to treat a variety of tumors including nasopharyngeal carcinoma.[51-53] The chemotherapy effect of PTX and PEG-PTX NPs towards NPC43 cells was tested by thiazolyl blue tetrazolium bromide (MTT) assays. The cytotoxicity of PTX and PEG-PTX NPs was time- and concentration-dependent as shown in Figure. 2d. As time and concentration increased, the cell viability decreased after the NPC43 cells were treated with PTX or PEG-PTX NPs, which indicated that PEG-PTX NPs could be effective to treat NPC43 cells. When the treatment incubation time was 16 h, small molecule PTX was more toxic to NPC43 cells compared with PEG-PTX NPs because PTX possessed direct drug effect but PEG-PTX NPs required time to release PTX to cells. However, as incubation time was extended to 64 h, both PEG-PTX NPs and PTX possessed similar chemotherapy effect towards NPC43 cells, which meant PEG-PTX NPs was an effective anticancer nanomedicine.

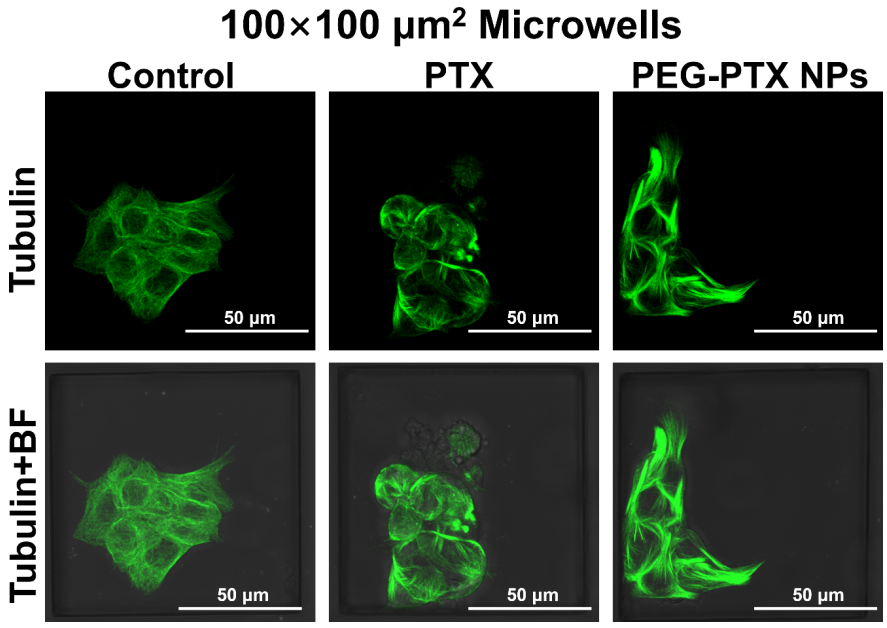

Figure 3 . Confocal laser scanning micrographs of NPC43 cells incubated with PTX and PEG-PTX NPs for 16 h in 100×100 μm^2 microwells. Tubulin in cells was stained by tubulin-tracker green (green fluorescence), and overlays of tubulin and bright field (BF) images.

For its therapeutic effect, PTX can promote the assembly and polymerization of tubulin, which will result in inhibition of mitosis and motility. Hence, after NPC43 cells were seeded in PDMS microwells and treated with PTX or PEG-PTX NPs for 16 h, the microtubules of NPC43 cells were marked by tubulin-tracker green assays. The concentrations of PTX and PEG-PTX NPs used were 5.85 nmol/mL for all subsequent experiments. As shown in **Figure. 3** , NPC43 cells in 100×100 μm^2 microwells without any treatment, as a control group, showed uniform and network-like green fluorescence, which exhibited that microtubules in the control group possessed well-organized and reticular distribution to maintain the stretched shape of cells. However, after the NPC43 cells were treated with PTX for 16 h, they became rounded, and microtubules were assembled together to show a bright and heterogeneous green fluorescence. For cells treated with PEG-PTX NPs for 16 h, bright green fluorescence of the tubulin bundles was observed because microtubules were gathered into large cluster but some cells still had elongated shape. In addition, the microtubules of NPC43 cells in 50×50 μm^2 microwells and 150×150 μm^2 microwells as shown in Supporting Figure. S1-S2 were also stained with green fluorescence. There was no difference for morphologic change of microtubules in microwells with different sizes. These results showed that PTX could be released from PEG-PTX NPs to act on intracellular microtubules, and PTX was more toxic than PEG-PTX NPs for NPC43 cells.

To further evaluate the effect of the microwell size and the degree of the confinement on the cytotoxicity of PTX and PEG-PTX NPs, the percentage of cell division and cell disruption were calculated as they represented the cellular activity and cell death. After NPC43 cells were seeded in the microwells and incubated with PTX or PEG-PTX NPs, a glass cover was placed on the top of the microwells to provide the additional confinement and limit the exchange of nutrients and drugs between the microwells and the outside surrounding. Six 3D platforms with 50×50, 100×100, and 150×150 μm^2 microwells without and with the cover were used to evaluate the cytotoxicity of PTX and PEG-PTX NPs. At first, the effect of the cover on cell proliferation was presented by the percentage of cell division. As shown in Supporting Figure. S3, after NPC43 cells were incubated for 16 h without any drug treatment, cells could divide in all microwells without and with covers. Furthermore, the percentage of cell division was calculated as shown in Supporting Fig. S4 and Table S1, which exhibited that the cell division was inhibited in microwells with covers. But the size of microwells did not affect cell proliferation because the percentages of cell division were similar for 50×50, 100×100, and 150×150 μm^2microwells without (˜11%) and with (˜7%) covers. There was no cell division after cells were treated with PTX or PEG-PTX NPs because drugs inhibit mitosis.

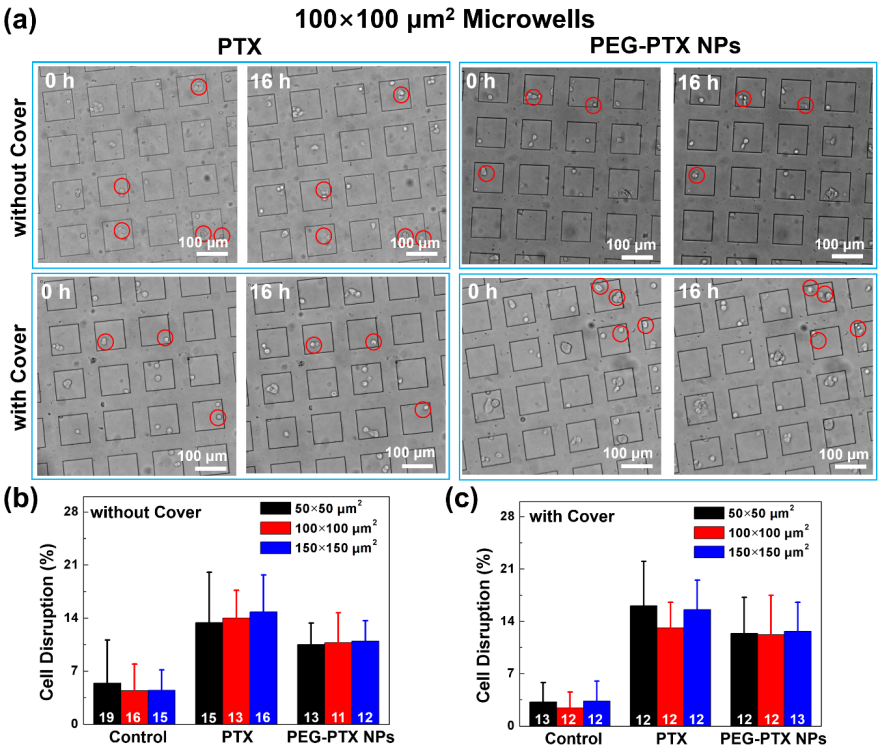

Figure 4 . Comparison of NPC43 cell disruption ratio with different treatments. (a) Optical images of NPC43 cells incubated with PTX and PEG-PTX NPs for 16 h in 100×100 μm^2 microwells without and with glass cover. Cell disruption was highlighted in red circles. Percentage of cell disruption after PTX and PEG-PTX NPs addition for 16 h in different microwells (b) without cover and (c) with cover. Number of NPC43 cells counted is marked in white.

To study the cytotoxicity of PTX and PEG-PTX NPs, the percentage of cell disruption was calculated as shown in Supporting Table S2. As shown in**Figure. 4a** and Supporting Figure. S5-S6, some cells ruptured after NPC43 cells were treated with PTX or PEG-PTX NPs for 16 h in microwells with different sizes. As shown in Figure. 4b-c, the size of microwells had no effect on cell division. Therefore 100×100 μm^2 microwells were used for further explanation. In 100×100 μm^2 microwells without a cover, the percentages of cell disruption after PTX and PEG-PTX NPs addition for 16 h were 14.01±3.66% and 10.77±3.92%, respectively. However, the percentage of cell disruption was only 4.42±3.50% for cells without any treatment. This result showed that PTX was more effective to treat NPC43 cells than PEG-PTX NPs, which was consistent with the result from the MTT assays. Furthermore, in 100×100 μm^2 microwells with a cover, the percentages of cell disruption after PTX and PEG-PTX NPs addition for 16 h were 13.12±3.44 and 12.23±5.26%, respectively. After NPC43 cells were treated with PEG-PTX NPs for 16 h, slightly more cells reptured in microwells with a cover compared to microwells without a cover. In the presence of PEG-PTX NPs, the additional confinement by the cover led to an increase in cell disruption. In addition, similar results were obtained for 50×50 and 150×150 μm^{2}microwells.

2.3. NPC43 cell behaviors with PTX and PEG-PTX NPs treatments

Because cell migration speed is a key indicator for cell behaviors and PTX could inhibit cell motility, cell migration speed was monitored after cells were treated with PTX and PEG-PTX NPs in different microwells. Additionally, cells on flat surface were also tested for comparison. As shown in Supporting Figure. S7, for cells without any treatment, the migration speed of NPC43 cells decreased a little in 16 h. However, after

NPC43 cells were incubated with PTX, the migration speed decreased to 0.1 μm/min after PTX treatment for 5.4 h. The time when the cell migration speed was equal to 0.1 μm/min was defined as $t_{0.1}$. NPC43 cells moved slower after treated with PTX for 5.4 h because small molecule PTX could act directly on tubulin to inhibit cell movement. However, for cells treated with PEG-PTX NPs, $t_{0.1}$ was 12.4 h which demonstrated that PEG-PTX NPs could continuously release PTX to slow down the NPC43 cell motility.

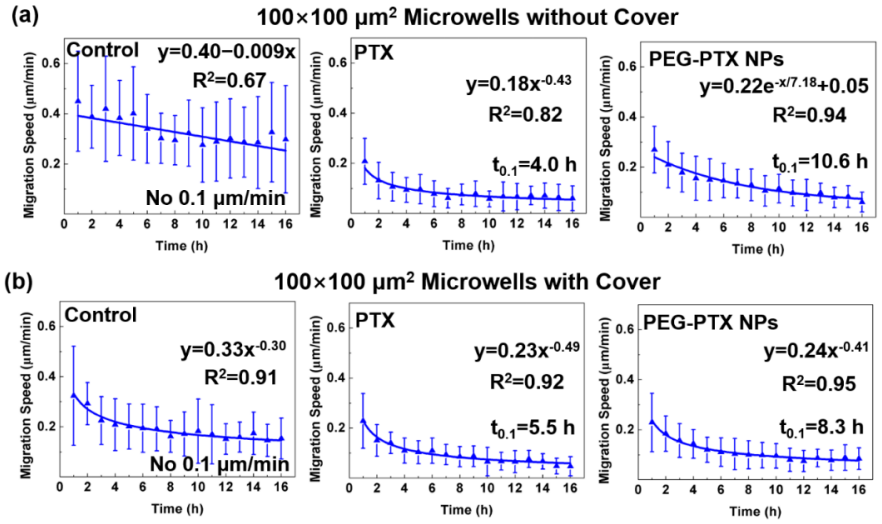

Figure 5 . Trends of NPC43 cell migration speed in 100×100 μm^2 microwells (a) without cover and (b) with cover after different treatments. These groups include control without any treatment, NPC43 cells treated with PTX, and NPC43 cells treated with PEG-PTX NPs. $t_{0.1}$ represents time when migration speed was equal to 0.1 μm/min.

NPC43 cell migration speed in different microwells without and with the covers are shown in **Figure. 5** and Supporting Figure. S8-S9. 100×100 μm^2 microwells were used for further explanation because the trends of NPC43 cell migration speed were similar for different microwell sizes after the same treatment. As shown in Figure. 5a, in 100×100 μm^2 microwells without a cover, cell migration speed for cells treated with PTX for 16 h decreased quickly, and the $t_{0.1}$ was 4.0 h. On the other hand, cell migration speed decreased continuously and $t_{0.1}$ was 10.6 h after the NPC43 cells were treated with PEG-PTX NPs. However, in 100×100 μm^2 microwells with covers, the migration speed fell to 0.2 μm/min in the first 5 h then the migration speed decreased very slowly in following 11 h for the control group without any drug treatment as shown in Figure. 5b. The trends of migration speed in microwells with covers were similar to the trends in microwells without covers after NPC43 cells were treated with PTX for 16 h. However, the trends of migration speed were different in microwells without and with covers after the NPC43 cells were treated with PEG-PTX NPs for 16 h and two different curves were required to fit their trends. After the cells were treated with PEG-PTX NPs, the migration speed fell fast in the first several hours, then maintained a very slow decline when cells were in microwells with covers. Hence, $t_{0.1}$for cells treated with PEG-PTX NPs in 100×100 μm^{2}microwells with covers was 8.3 h, which was 2.3 h less than $t_{0.1}$ for cells treated with PEG-PTX NPs in 100×100 μm^2 microwells without covers. These results demonstrated that the covers provided additional confinement and would decrease the migration speed of NPC43 cells. Cells treated with small molecule anticancer drug PTX and PEG-PTX NPs showed different trends of cell migration speed. In 50×50 μm^2 and 150×150 μm^2 microwells, similar drug induced cell migration speed reduction was obtained as shown in Supporting Figure. S8-S9.

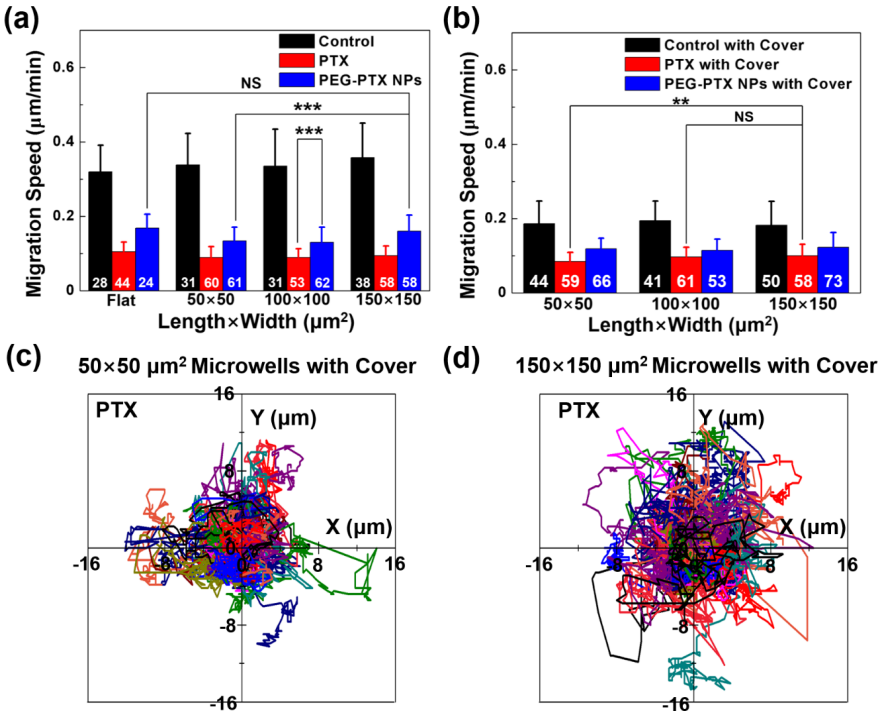

Figure 6 . NPC43 cell migration behavior in microwells without and with cover. (a) Migration speed of NPC43 cells with PTX and PEG-PTX NPs treatments over 16 h in microwells (a) without cover and (b) with cover. Cell migration trajectories of NPC43 cells over 16 h with PTX added in (c) 50×50 μm^2 microwells with cover and (d) 150×150 μm^2 microwells with cover. Starting points of cell migration trajectories are (0, 0). One-way ANOVA and Tukey's post hoc tests, NS – not significant, **p <0.01, and ***p <0.001. Number of NPC43 cells counted is marked in white.

Average migration speed of NPC43 cells on flat surface and in different microwells are as shown in Supporting Table S3. As shown in**Figure. 6a** , without any treatment, the average migration speeds of cells on the flat surface and in different microwells without covers were similar with speed over 0.3 μm/min. After the NPC43 cells were treated with PTX or PEG-PTX NPs for 16 h, the average migration speed decreased significantly. Especially, the average migration speed was only about 0.1 μm/min after NPC43 cells were treated with PTX. The average migration speed of cells treated with PEG-PTX NPs was faster compared to cells treated with PTX NPs because PTX was more effective than PEG-PTX NPs to treat NPC43 cells in 16 h. After the cells were treated with PEG-PTX NPs in 150×150 μm^2 microwells for 16 h, the average migration speed was 0.16±0.04 μm/min. But the average migration speed was 0.13±0.04 μm/min for cells in 50×50 μm^2 microwells with the same treatment, indicating that NPC43 cells treated with PEG-PTX NPs possessed a faster speed in larger microwells. Furthermore, the average migration speed was also calculated in microwells with covers as shown in Figure. 6b. The cover decreased the migration speed because the cover inhibited the exchange of nutrients which made the cells unhealthy. For control groups, the average migration speeds were about 0.20 μm/min in all microwells with covers, which were slower than those in microwells without covers with speed over 0.3 μm/min. In microwells with covers, NPC43 cells treated with PTX still possessed the slowest speed among other groups including control without any treatment and NPC43 cells treated with PEG-PTX NPs. However, for the NPC43 cells treated with PTX, there was no difference for the average migration speed in microwells without and with covers as shown in Supporting Figure. S10a. The reason might be the additional confinement by the cover limited the supply of PTX into the microwells and slightly decreased the cytotoxicity, but PTX was still toxic enough to decrease the migration speed. It was a balance of PTX toxicity and the effect of 3D confinement.

After the NPC43 cells were treated with PTX, $t_{0.1}$ for microwells with covers was larger than $t_{0.1}$ for microwells without covers as shown in Figure. 5 and Supporting Figure. S12-S13. For the NPC43 cells treated with PEG-PTX NPs in microwells with covers, the average speed was lower than those in microwells without covers, especially in 150×150 μm^2 microwells as shown in Supporting Figure. S10b. For the NPC43 cells in 150×150 μm^2 microwells without covers, PEG-PTX NPs needed a longer time to release PTX and inhibit cell movement, with $t_{0.1}$ of 12.9 h as shown in Supporting Figure. S9a. In addition, the cover decreased the migration speed in the first 5 h. So it was a combination effect of nanomedicine and the confinement that caused the decrease in the migration speed. The trajectories of NPC43 cells without any drug treatment and treated with PTX in 50×50 and 150×150 μm^2 microwells are shown in Supporting Figure. S11 and Figure. 6c-d, respectively. As shown in Supporting Figure. S11, in microwells with covers, the moving range of NPC43 cells without any drug treatment was smaller than that in microwells without covers. But there was no difference for the moving range of NPC43 cells without any drug treatment in microwells with different sizes. After the NPC43 cells were treated with PTX as shown in Figure. 6c-d, the moving range was reduced. In addition, the moving range of cells in 150×150 μm^{2}microwells was slightly bigger than that in 50×50 μm^{2}microwells as shown in Figure. 6b-c. Cells without any treatment were healthy and possessed normal speed to move and change directions. In complete confinement with covers on top of microwells, the speed of cells decreased and cells could not move as far as cells in microwells without covers. After cells were treated with PTX, cells were too unhealthy to move or change directions. In smaller microwells, it was easier for the NPC43 cells treated with PTX to touch the sidewalls of the microwells, and the cells could not move further, leading to a smaller moving range.

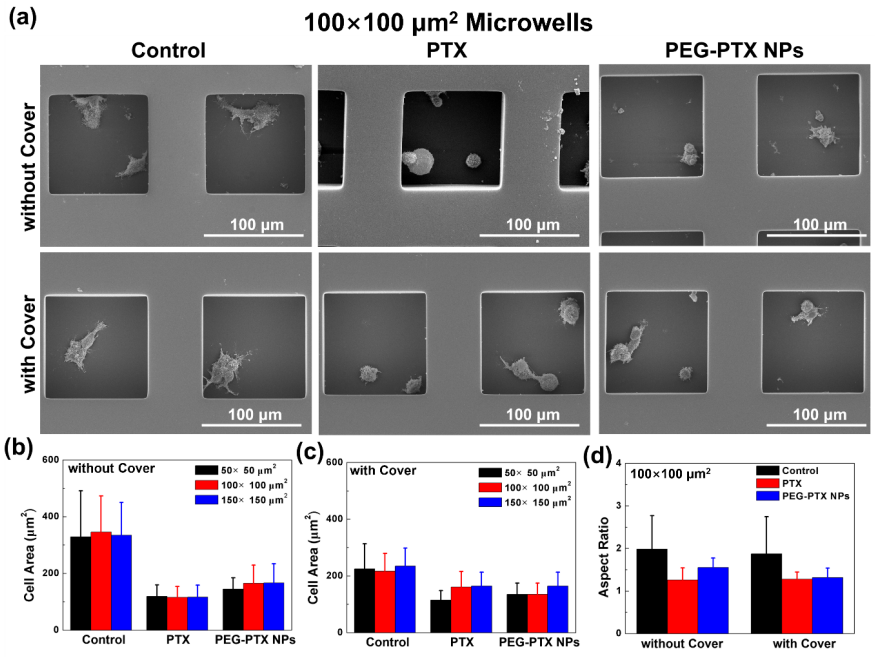

Figure 7 . NPC43 cell morphology after various treatments. (a) Scanning electron micrographs of NPC43 cells with PTX and PEG-PTX NPs added over 16 h in 100×100 μm^2 microwells without and with cover. Cell area after cells treated with PTX and PEG-PTX NPs for 16 h in microwells (b) without cover and (c) with cover. (d) Cell aspect ratio after NPC43 cells treated with PTX and PEG-PTX NPs for 16 h in 100×100 μm^2 microwells without and with cover. Number of NPC43 cells counted is marked in white.

At last, the morphology of NPC43 cells in microwells was obtained by SEM. As shown in **Figure. 7** and Supporting Figure. S12-13, for the NPC43 cells without any treatment in microwells without and with covers, they elongated and had many extended filopodia. However, the NPC43 cells became rounded and

had few filopodia after treatment with PTX for 16 h. And the NPC43 cells treated with PEG-PTX NPs were elliptical with a few filopodia. To analyze the change of the cell morphology, the cell area and aspect ratio were evaluated as shown in Supporting Tables S4-S5. As shown in Figure. 7b, the NPC43 cells without any treatment possessed the largest cell area and the NPC43 cells treated with PTX had the smallest cell area. Cell area for the nPC43 cells treated with PEG-PTX NPs was slightly larger than the NPC43 cells treated with PTX. In microwells with covers, the cell area was about 200 μm^2 as shown in Figure. 7c, which was smaller than the cell area of over 300 μm^2 for the NPC43 cells in microwells without covers. Cell area was similar for the NPC43 cells treated with PTX and PEG-PTX NPs. In 100×100 μm^2microwells, the cell area was 345±127 μm^2 for control without covers, 115±39 μm^2 for PTX without covers, 165±64 μm^2 for PEG-PTX NPs without covers, 216±63 μm^2 for control with covers, 139±44 μm^2 for PTX with covers, and 135±44 μm^2 for PEG-PTX NPs with covers. Furthermore, the aspect ratio of cells, which illustrated the cell elongation, was calculated. As shown in Figure. 7d, in 100×100 μm^2microwells, the aspect ratios were 1.98±0.78 for control without covers, 1.26±0.28 for PTX without covers, 1.55±0.22 for PEG-PTX NPs without covers, 1.87±0.87 for control with covers, 1.27±0.17 for PTX with covers, and 1.36±0.23 for PEG-PTX NPs with covers. These results were consistent with the average speed dependence on the microwell size and the presence of the cover. For the control group without covers, the NPC43 cells moved normally and the cells elongated with the highest aspect ratio. After being treated with PTX, the NPC43 cells became rounded, and the aspect ratio was the lowest. Supporting Figure. S14 shows that in 50×50 and 150×150 μm^2 microwells, similar results were obtained, independent of the size of the microwells.

3. Conclusion

In this work, 3D microwells without and with covers were fabricated to study the interplay of the cytotoxicity from PEG-PTX NPs and cell behaviors. First, stable PEG-PTX NPs with about 110 nm diameter were successfully synthesized to treat NPC43 cells. At short time, small molecule drug PTX was more effective to treat NPC43 cells than PEG-PTX NPs. After 64 h of treatment, the effect was similar according to results from the MTT assays. When the microwells had covers on the top, they provided additional confinement, and the cell division was slightly inhibited. In microwells with covers, more cell disruption was observed than those in microwells without covers after the NPC43 cells were treated with PEG-PTX NPs. In microwells without and with covers, more cell disruption was found when the NPC43 cells were treated with PTX than the NPC43 cells treated with PEG-PTX NPs. In addition, the cell migration speed decreased in microwells with covers. After cells were treated with PTX or PEG-PTX NPs, the cell migration speed further reduced. The effect of drug formations, microwells confinement, and size of microwells on cell behaviors including the cell migration speed, cell area, and cell elongation were studied in detail. In microwells without and with covers, after the NPC43 cells were treated with PTX, the migration speed was the lowest among other groups including control without any treatment, and NPC43 cells treated with PEG-PTX NPs. For cells treated with PEG-PTX NPs in microwells with covers, the average speed was lower than those in microwells without the cover, especially in 150×150 μm^2 microwells. Furthermore, cell area decreased when the NPC43 cells were in microwells with covers. After cells were treated with PTX or PEG-PTX NPs, cell area further decreased, and their aspect ratio reduced. NPC43 cells became smaller and more rounded after treatment with PTX, while they had the elliptical shape after treatment with PEG-PTX NPs. This work provides a new approach to evaluate the relationship between nanomedicine, 3D confinement, and cell behaviors *in vitro* .

4. Experimental Section/Methods

Materials : Polydimethylsiloxane (PDMS) pre-polymer was purchased from Dow. Trichloro (1H , 1H , 2H , 2H -perfluorooctyl) silane (FOTS) was purchased from J&K. Tetrahydrofuran (THF) and dimethylformamide (DMF) were purchased from Sigma. Paclitaxel was purchased from Xi'an Haoxuan Biological Technology Co., Ltd. PEGylated (methoxypolyethylene glycol 2000) paclitaxel (PEG-PTX) was synthesized according to the previous literature.[48-50] Tubulin-tracker green and thiazolyl blue tetrazolium bromide (MTT) assays were purchased from Beyotime.

Characterization: The diameter and size distribution of PEG-PTX NPs were measured by dynamic light

scattering (Zeta-sizer Nano, Malvern). The migration of cells, cell division, and cell disruption were recorded by a Nikon Eclipse upright microscope. The fluorescence of tubulin in cells was measured by a confocal laser scanning microscope (TCS SP5, Leica). The morphologies of microwells, nanoparticles, and cells were measured by a scanning electron microscope (SU5000 FE, Hitachi). The absorbance at 490 nm was measured by a Bio-Rad 680 microplate reader to calculate cell viability. The migration speed, migration trajectories, cell area, and aspect ratio of cells were calculated by Image J software. To calculate the aspect ratio of the cell shape, an ellipse was fitted over the cell with a short axis a and a long axis b , so that aspect ratio was obtained by b/a .

Fabrication of Microwell Arrays: PDMS microwells arrays were fabricated according to our previous work.[47] Si was used to fabricate the mold of microwell arrays. Microwells were patterned on Si wafer using photolithography with AZ6130 as the photoresist. 50 μm tall pillars in Si was etched in a deep reactive ion etching system. The etch conditions included repeated 7 s passivation cycle with 85 sccm C_4F_8, 600 W coil power at 20 mTorr, and 14 s etch cycle with 130 sccm SF_6, 600 W coil power, 20 W platen power at 40 mTorr. 34 alternative cycles were applied to fabricate the 50 μm tall pillars. A monolayer of FOTS was coated on the Si mold as anti-stiction layer. The PDMS prepolymer with a 10:1 base to curing agent ratio was cast on the Si mold, spin coated at 1000 rpm for 1 min, and cured at 80 °C overnight. Replicated microwell arrays were then peeled off from the Si mold for further process.

Synthesis of PEG-PTX NPs: Similar method was reported in our previous work.[54-56] Briefly, PEG-PTX (40 mg) was dissolved in THF (5 mL), and dropwise added into water (10 mL) under stirring. After THF were completely evaporated, PEG-PTX NPs were collected.

Cell culture: NPC43 cells[57-60] were cultured in Roswell Park Memorial Institute 1× 1640 medium (Gibco) with 10% fetal bovine serum (FBS, Gibco), 0.2% 2 mM rock inhibitor Y-27632 (ENZO), and 1% antibiotic antimycotic (Gibco). NPC43 cells were maintained in incubator at 37 °C with 5% CO_2. The medium was changed every two days and the cells were passaged when they reached 70% confluency.

Cell viability assays: The MTT assays against NPC43 cells were carried out. Similar experimental process was shown in our previous work.[61, 62] Briefly, PTX and PEG-PTX NPs were added into cell culture medium with different concentrations. NPC43 cells were incubated with PTX and PEG-PTX NPs for 16, 40, and 64 h.

Time-lapse imaging: Microwell platforms with different sizes were bonded to a confocal dish using O_2 plasma. After twice sterilization with 70% ethanol, the confocal dish with platforms was put in a plasma system and treated with 5 min O_2 plasma to form a hydrophilic surface. The O_2 plasma conditions were 20 sccm flow rate, 100 mTorr chamber pressure, and 100 W RF power. The dish was maintained in 1× phosphate buffered saline (PBS) before cell seeding. A total number of 10^5 NPC43 cells were seeded in the dish for each experiment and maintained in cell culture medium for 8 h incubation. After that, the medium was changed to a mixture of 1:1 complete cell culture medium and CO_2independent medium (Gibco) supplemented with 10% FBS, 1% antibiotic antimycotic, and 1% 100× GlutaMax (Gibco). Then PTX (5.85 nmol/mL) or PEG-PTX NPs (5.85 nmol/mL) was added. A Nikon Eclipse upright microscope was used to capture cell movements for 16 h at 5 min intervals.

Cell preparation for scanning electron microscopy: Cells on platforms were washed by PBS twice and fixed by 4% paraformaldehyde for 15 min. The cells were then treated by ethanol with concentration of 30%, 50%, 70%, 80%, 90%, 95%, and 100% for 5 min each, and then dried in a critical point dryer (EM CPD300, Leica) for 4 h. The dried samples were coated with a thin layer of Au to avoid charging and placed in a scanning electron microscope (SEM) for imaging.

Supporting Information

Supporting Information is available from the Wiley Online Library or from the author.

Acknowledgements

Wenhai Lin and Yuanhao Xu contributed equally. This work was supported by the Center for Biosystems, Neuroscience, and Nanotechnology (CBNN) of City University of Hong Kong (9360148, 9380062) and the University Grants Council of Hong Kong (GRF Projects: 11212519, 11207620, and 11207821). We gratefully appreciate members of CBNN and cleanroom technical staff for their help.

Received: ((will be filled in by the editorial staff)) Revised: ((will be filled in by the editorial staff)) Published online: ((will be filled in by the editorial staff))

References

[1] J. W. M. Crawley, I. E. Gow, N. Lawes, I. Kowalec, L. Kabalan, C. R. A. Catlow, A. J. Logsdail, S. H. Taylor, N. F. Dummer, G. J. Hutchings, *Chem. Rev.* **2022** , *122* , 6795.

[2] W. R. Algar, M. Massey, K. Rees, R. Higgins, K. D. Krause, G. H. Darwish, W. J. Peveler, Z. Xiao, H.-Y. Tsai, R. Gupta, K. Lix, M. V. Tran, H. Kim, *Chem. Rev.* **2021** , *121* , 9243.

[3] Z. Meng, R. M. Stolz, L. Mendecki, K. A. Mirica, *Chem. Rev.* **2019** , *119* , 478.

[4] G. Chen, I. Roy, C. Yang, P. N. Prasad, *Chem. Rev.***2016** , *116* , 2826.

[5] H. D. Lawson, S. P. Walton, C. Chan, *ACS Appl. Mater. Interfaces* **2021** , *13* , 7004.

[6] Y. Cai, X. Chen, J. Si, X. Mou, X. Dong, *Small***2021** , *17* , 2103072.

[7] W. Lin, D. Colombani-Garay, L. Huang, C. Duan, G. Han,*WIREs Nanomed. Nanobiotechnol.* **2020** , *14* , 1627.

[8] S. Kulkarni, A. Pandey, S. Mutalik, *Nanomed. Nanotechnol. Biol. Med.* **2020** , *26* , 102175.

[9] X. Wang, W. Lin, W. Zhang, C. Li, T. Sun, G. Chen, Z. Xie,*J. Colloid Interface Sci.* **2019** , *536* , 208.

[10] I. de Lazaro, D. J. Mooney, *Nat. Mater.* **2021** ,*20* , 1469.

[11] J. Wang, Y. Li, G. Nie, *Nat. Rev. Mater.* **2021** , 1.

[12] G. Li, B. Sun, Y. Li, C. Luo, Z. He, J. Sun, *Small***2021** , *17* , 2101460.

[13] E. S. Lee, J. M. Shin, S. Son, H. Ko, W. Um, S. H. Song, J. A. Lee, J. H. Park, *Adv. Healthcare Mater.* **2019** , *8* , 1801320.

[14] L. Leggio, G. Arrabito, V. Ferrara, S. Vivarelli, G. Paterno, B. Marchetti, B. Pignataro, N. Iraci, *Adv. Healthcare Mater.***2020** , *9* , 2000731.

[15] M. A. Subhan, V. P. Torchilin, *Nanomed. Nanotechnol. Biol. Med.* **2020** , *29* , 102239.

[16] F. Chen, G. Hableel, E. R. Zhao, J. V. Jokerst, *J. Colloid Interface Sci.* **2018** , *521* , 261.

[17] R. Zheng, Y. Liu, B. Yu, L. Zhao, N. Yang, A. Chen, L. Xu, H. Cheng, X. Jiang, S. Li, *J. Colloid Interface Sci.* **2022** ,*622* , 298.

[18] H. Hu, N. F. Steinmetz, *Biotechnol. J.* **2020** ,*15* , 2000077.

[19] J. W. M. Osterrieth, D. Fairen-Jimenez, *Biotechnol. J.***2021** , *16* , 2000005.

[20] J. Parra-Nieto, M. A. G. Del Cid, I. A. de Carcer, A. Baeza,*Biotechnol. J.* **2021** , *16* , 2000150.

[21] J. Shi, P. W. Kantoff, R. Wooster, O. C. Farokhzad, *Nat. Rev. Cancer* **2016** , *17* , 20.

[22] Y. Min, J. M. Caster, M. J. Eblan, A. Z. Wang, *Chem. Rev.* **2015** , *115* , 11147.

[23] N. K. Ibrahim, N. Desai, S. Legha, P. Soon-Shiong, R. L. Theriault, E. Rivera, B. Esmaeli, S. E. Ring, A. Bedikian, G. N. Hortobagyi, J. A. Ellerhorst, *Clin. Cancer Res.* **2002** ,*8* , 1038.

[24] N. Desai, V. Trieu, Z. W. Yao, L. Louie, S. Ci, A. Yang, C. L. Tao, T. De, B. Beals, D. Dykes, P. Noker, R. Yao, E. Labao, M. Hawkins, P. Soon-Shiong, *Clin. Cancer Res.* **2006** , *12* , 1317.

[25] T.-Y. Kim, D.-W. Kim, J.-Y. Chung, S. G. Shin, S.-C. Kim, D. S. Heo, N. K. Kim, Y.-J. Bang, *Clin. Cancer Res.* **2004** ,*10* , 3708.

[26] S. C. Kim, D. W. Kim, Y. H. Shim, J. S. Bang, H. S. Oh, S. W. Kim, M. H. Seo, *J. Controlled Release* **2001** , *72* , 191.

[27] S.-E. Kim, H. Kim, J. Doh, *Lab Chip* **2019** ,*19* , 2009.

[28] E. Forslund, K. Guldevall, P. E. Olofsson, T. Frisk, A. E. Christakou, M. Wiklund, B. Onfelt, *Front. Immunol.* **2012** ,*3* , 300.

[29] Y. Xia, H. Chen, J. Li, H. Hu, Q. Qian, R. X. He, Z. Ding, S. S. Guo, *ACS Appl. Mater. Interfaces* **2021** , *13* , 23489.

[30] L. Sun, J. Guo, H. Chen, D. Zhang, L. Shang, B. Zhang, Y. Zhao,*Adv. Sci.* **2021** , *8* , 2100126.

[31] H. Lu, M. H. Stenzel, *Small* **2018** , *14* , 1702858.

[32] W. Li, J. Liu, L. Chen, W. Wei, K. Qian, Y. Liu, J. Leng,*Small* **2022** , *18* , e2105958.

[33] M. G. Barbato, R. C. Pereira, H. Mollica, A. Palange, M. Ferreira, P. Decuzzi, *J. Colloid Interface Sci.* **2021** ,*594* , 409.

[34] E. Prince, S. Kheiri, Y. Wang, F. Xu, J. Cruickshank, V. Topolskaia, H. Tao, E. W. K. Young, A. P. McGuigan, D. W. Cescon, E. Kumacheva, *Adv. Healthcare Mater.* **2022** , *11* , e2101085.

[35] H. J. An, H. S. Kim, J. A. Kwon, J. Song, I. Choi, *ACS Appl. Mater. Interfaces* **2020** , *12* , 6924.

[36] J. Lee, G. D. Lilly, R. C. Doty, P. Podsiadlo, N. A. Kotov,*Small* **2009** , *5* , 1213.

[37] P. Datta, L. Meli, L. Li, N. Migliore, E. Schaefer, S. T. Sharfstein, J. S. Dordick, R. J. Linhardt, *Biotechnol. J.***2014** , *9* , 386.

[38] J. Choi, E. K. Lee, J. Choo, J. Yuh, J. W. Hong,*Biotechnol. J.* **2015** , *10* , 1682.

[39] A. Kletzmayr, F. Clement Frey, M. Zimmermann, D. Eberli, C. Millan, *Biotechnol. J.* **2020** , *15* , 1900439.

[40] T. Y. Tu, Z. Wang, J. Bai, W. Sun, W. K. Peng, R. Y. J. Huang, J. P. Thiery, R. D. Kamm, *Adv. Healthcare Mater.* **2014** ,*3* , 609.

[41] Y. W. Hu, X. Z. Sui, F. Song, Y. Q. Li, K. Y. Li, Z. Y. Chen, F. Yang, X. Y. Chen, Y. H. Zhang, X. N. Wang, Q. Liu, C. Li, B. B. Zou, X. F. Chen, J. Wang, P. Liu, *Nat. Commun.* **2021** ,*12* , 2581.

[42] C. H. Kim, I. R. Suhito, N. Angeline, Y. Han, H. Son, Z. Luo, T. H. Kim, *Adv. Healthcare Mater.* **2020** , *9* , 1901751.

[43] J. L. Zhuang, J. Zhang, M. H. Wu, Y. Q. Zhang, *Adv. Sci.***2019** , *6* , 1901462.

[44] A. Kang, H. I. Seo, B. G. Chung, S. H. Lee, *Nanomed. Nanotechnol. Biol. Med.* **2015** , *11* , 1153.

[45] Y. H. Xu, S. F. Zhou, Y. W. Lam, S. W. Pang, *Front. Immunol.* **2017** , *8* , 998.

[46] Y. J. Yamanaka, C. T. Berger, M. Sips, P. C. Cheney, G. Alter, J. C. Love, *Integr. Biol.* **2012** , *4* , 1175.

[47] Y. Xu, S. W. Pang, *Lab Chip* **2019** , *19* , 2466.

[48] J. Lu, X. Chuan, H. Zhang, W. Dai, X. Wang, X. Wang, Q. Zhang,*Int. J. Pharm.* **2014** , *471* , 525.

[49] H. Sun, Q. Zhang, Z. Zhang, J. Tong, D. Chu, J. Gu, *J. Pharm. Biomed. Anal.* **2017** , *145* , 255.

[50] H. Zhang, H. Hu, H. Zhang, W. Dai, X. Wang, X. Wang, Q. Zhang,*Nanoscale* **2015** , *7* , 10790.

[51] T. Zhou, Y. Yang, S. Ma, L. Lin, T. Zhou, C. Zhang, X. Ding, R. Wang, G. Feng, Y. Chen, R. Xu, Y. Huang, L. Zhang, *ESMO Open***2021** , *6* , 100313.

[52] S. L. Liu, X. S. Sun, X. Y. Li, Q. Y. Chen, H. X. Lin, Y. F. Wen, S. S. Guo, L. T. Liu, H. J. Xie, Q. N. Tang, Y. J. Liang, J. J. Yan, C. Lin, Z. C. Yang, L. Q. Tang, L. Guo, H. Q. Mai, *BMC Cancer* **2018** , *18* , 1279.

[53] Q. Pei, X. Hu, S. Liu, Y. Li, Z. Xie, X. Jing, *J. Controlled Release* **2017** , *254* , 23.

[54] W. Lin, T. Sun, Z. Xie, J. Gu, X. Jing, *Chem. Sci.***2016** , *7* , 1846.

[55] Y. Zhu, W. Lin, W. Zhang, Y. Feng, Z. Wu, L. Chen, Z. Xie,*Chin. Chem. Lett.* **2017** , *28* , 1875.

[56] W. Lin, W. Zhang, S. Liu, Z. Li, X. Hu, Z. Xie, C. Duan, G. Han, *ACS Appl. Mater. Interfaces* **2019** , *11* , 43928.

[57] C. M. Tsang, Z. Y. Liu, W. Zhang, C. You, G. E. Jones, S. W. Tsao, S. W. Pang, *Acta Biomater.* **2020** , *101* , 168.

[58] W. G. Zhang, Z. Y. Liu, S. W. Pang, *Biotechnol. Bioeng.***2021** , *118* , 1444.

[59] B. P. Lam, S. K. C. Cheung, Y. W. Lam, S. W. Pang, *RSC Adv* **2020** , *10* , 28975.

[60] Z. Liu, W. Zhang, S. W. Pang, *Biosci. Rep.***2020** , *40* , 20194113.

[61] W. Lin, L. Yin, T. Sun, T. Wang, Z. Xie, J. Gu, X. Jing,*Biomacromolecules* **2018** , *19* , 1625.

[62] W. Lin, X. Guan, T. Sun, Y. Huang, X. Jing, Z. Xie,*Colloids Surf. B* **2015** , *126* , 217.

3D microwells without and with covers were fabricated to evaluate the relationship between the cytotoxicity from PEGylated paclitaxel nanomedicine and nasopharyngeal carcinoma cell behaviors such as cell proliferation, cell migration speed, cell elongation, and cell spreading area. This is the first work to study the cytotoxicity of nanomedicine and cell behaviors in 3D confinement with the cover on top.

Dr. W. Lin, Dr. Y. Xu, X. Hong, and Prof. S. W. Pang*

PEGylated Paclitaxel Nanomedicine Meets 3D Confinement: Cytotoxicity and Cell Behaviors